LATERAL BRANCHING OXIDOREDUCTASE, one novel target gene of Squamosa Promoter Binding Protein-like 2, regulates tillering in switchgrass

Ruijuan Yang[1,2]*, Wenwen Liu[1]*, Ying Sun[1], Zhichao Sun[1], Zhenying Wu[1,2], Yamei Wang[1], Mengqi Wang[1], Honglun Wang[3], Shiqie Bai[4] and Chunxiang Fu[1,2,3]

[1]Shandong Provincial Key Laboratory of Energy Genetics and CAS Key Laboratory of Biofuels, Qingdao Institute of Bioenergy and Bioprocess Technology, Chinese Academy of Sciences, Qingdao 266101, China; [2]University of Chinese Academy of Sciences, Beijing 100049, China; [3]CAS Key Laboratory of Tibetan Medicine Research, Northwest Institute of Plateau Biology, Chinese Academy of Sciences, Xining 810008, China; [4]Sichuan Academy of Grassland Science, Chengdu 611731, China

Author for correspondence:
Chunxiang Fu
Email: fucx@qibebt.ac.cn

Received: *25 November 2021*
Accepted: *29 March 2022*

New Phytologist (2022) **235:** 563–575
doi: 10.1111/nph.18140

Key words: *LATERAL BRANCHING OXIDOREDUCTASE*, miR156, SPL transcription factor, strigolactones, switchgrass, tillering.

Summary

- Strigolactones (SLs) play a critical role in regulating plant tiller number. *LATERAL BRANCHING OXIDOREDUCTASE* (*LBO*) encodes an important late-acting enzyme for SL biosynthesis and regulates shoot branching in *Arabidopsis*. However, little is known about the function of *LBO* in monocots including switchgrass (*Panicum virgatum* L.), a dual-purpose fodder and biofuel crop.
- We studied the function of *PvLBO* via the genetic manipulation of its expression levels in both the wild-type and miR156 overexpressing ($miR156_{OE}$) switchgrass. Co-expression analysis, quantitative real-time polymerase chain reaction (qRT-PCR), transient dual luciferase assay, and chromatin immunoprecipitation-qPCR were all used to determine the activation of *PvLBO* by miR156-targeted Squamosa Promoter Binding Protein-like 2 (PvSPL2) in regulating tillering of switchgrass.
- *PvLBO*transcripts dramatically declined in $miR156_{OE}$ transgenic switchgrass, and the overexpression of *PvLBO* in the $miR156_{OE}$ transgenic line produce fewer tillers than the control. Furthermore, we found that PvSPL2 can directly bind to the promoter of *PvLBO* and activate its transcription, suggesting that *PvLBO* is a novel downstream gene of PvSPL2.
- We propose that *PvLBO* functions as an SL biosynthetic gene to mediate tillering and acts as an important downstream factor in the crosstalk between the SL biosynthetic pathway and the miR156-SPL module in switchgrass.

Introduction

Strigolactones (SLs) are a class of carotenoid-derived plant hormones that primarily function as germination stimulants for root parasitic plants, symbiotic signals for fungi, and inhibitors of shoot branching/tillering (Cook *et al.*, 1966; Akiyama *et al.*, 2005; Gomez-Roldan *et al.*, 2008). Strigolactones are synthesized from all-*trans*-β-carotene by 9-*cis*-β-carotene isomerase DWARF27 (D27), CAROTENOID CLEAVAGE DIOXYGENASE 7 (CCD7/D17/MAX3, MORE AXILLARY GROWTH 3), and CAROTENOID CLEAVAGE DIOXYGENASE 8 (CCD8/D10/MAX4). These enzymes are known to convert β-carotene to carlactone (CL), which is then converted to carlactonoic acid (CLA) by the cytochrome P450 enzyme MORE AXILLARY GROWTH 1 (MAX1) (Booker *et al.*, 2005; Zhang *et al.*, 2014). The conversion of all-*trans*-β-carotene to CLA is highly conserved and is generally considered to be an important step in SL biosynthesis (Yoneyama *et al.*, 2018). However, the structures of SLs produced by subsequent steps after CLA synthesis vary across plant species (Yoneyama & Brewer, 2021). Compounds with an ABC-ring system, such as 4-deoxyorobanchol (4DO), 5-deoxystrigol (5DS), and orobanchol (ORO), are called canonical SLs, while SLs such as methyl carlactonoate (MeCLA) and hydroxymethyl carlactonoate (1′-HO-MeCLA) without typical ABC-rings belong to noncanonical SLs (Yoneyama *et al.*, 2009; Omoarelojie *et al.*, 2019).

Arabidopsis LATERAL BRANCHING OXIDOREDUCTASE (*LBO*) encodes a 2-oxoglutarate-dependent dioxygenase that oxidizes MeCLA to 1′-HO-MeCLA to act during the final steps of noncanonical SLs biosynthesis (Brewer *et al.*, 2016). Although most MeCLA is converted to CLA by LBO *in vitro*, 1′-HO-MeCLA is indeed present as an endogenous compound in *Arabidopsis* (Yoneyama *et al.*, 2020). Moreover, CL and MeCLA can accumulate in the roots of *Arabidopsis lbo* mutants, and the morphological characterizations induced by MeCLA accumulation

*These authors contributed equally to this work.

are intermediate between the wild-type Ws-4 and the *max4* mutant plants. Overexpression of *LBO* in Ws-4 plants cannot reduce branching (Brewer *et al.*, 2016). While the 1′-HO-MeCLA is highly unstable and difficult to detect in plants, the enzyme activity analysis of LBO recombinant proteins *in vitro* suggests that the conversion of MeCLA to 1′-HO-MeCLA is conserved in *Arabidopsis*, tomato, maize, and sorghum (Yoneyama *et al.*, 2020). Nevertheless, it remains unclear whether LBO regulates tiller bud outgrowth or shoot architecture in monocotyledons, especially perennial grasses.

Strigolactones are perceived by an α/β hydrolase, DWARF14 (D14) in rice (Chevalier *et al.*, 2014). Upon SL perception, D14 forms a complex with an F-box component DWARF 3 (D3) of the SCF E3 ubiquitin ligase complex and a repressor DWARF 53 (D53) of SL signaling, triggering the ubiquitination and degradation of D53, resulting in transcriptional changes of downstream genes (Zhou *et al.*, 2013). A similar interaction has been confirmed in *Arabidopsis* for the orthologs of D14, D3, and D53 (Zhou *et al.*, 2013). During this reaction, D14 is also degraded via proteolysis in response to SLs (Chevalier *et al.*, 2014). Other SL-responsive genes also have been identified as well, including SL biosynthetic genes, *MAX3*, *MAX4* and *SMXL2*, *SMXL6*, *SMXL7*, *SMXL8*, and anthocyanin biosynthetic activator genes, *PRODUCTION OF ANTHOCYANIN PIGMENT 1* (*PAP1*) and *MYB113* in *Arabidopsis* (Wang *et al.*, 2020); and the bud outgrowth repressor gene, *TEOSINTE BRANCHED 1* (*TB1*) and cytokinin oxidase/dehydrogenase gene, *CYTOKININ OXIDASE/DEHYDROGENASE 9* (*CKX9*) in rice (Lu *et al.*, 2013; Duan *et al.*, 2019).

Strigolactones have been shown to regulate plant branching, leaf shape and senescence, and root development (Braun *et al.*, 2012; Waldie *et al.*, 2014). Strigolactones can also regulate plant tolerance to drought, salt and phosphate starvation stresses as well as the biosynthesis of anthocyanin and flavonols (Mayzlish-Gati *et al.*, 2012; Waters *et al.*, 2017; Wang *et al.*, 2020). Aside from phytohormones, microRNA (miRNA) is another multi-function factor involved in plant growth and development, and biotic and abiotic stress responses in plants. Among them, miR156 is one of the conserved master regulators of plant vegetative phase transitions by suppressing its target *SQUAMOSA PROMOTER BINDING PROTEIN LIKE* (*SPL*) genes (Wu & Poethig, 2006). Overexpression of miR156 or the repression of its target *SPLs* in different plant species can result in severe decrease of apical dominance and produce obvious morphological changes, including increased tiller and leaf numbers, altered inflorescence architecture, accumulated anthocyanin, and reduced lignin content (Chuck *et al.*, 2007; Wang *et al.*, 2008; Miura *et al.*, 2010; Gou *et al.*, 2011; Fu *et al.*, 2012). *OsTB1* is an important negative regulator controlling the outgrowth of axillary buds in rice (Takeda *et al.*, 2003). Overexpression of *IDEAL PLANT ARCHITECTURE 1* (*IPA1*, otherwise known as *OsSPL14*), a key gene repressed by miR156, can decrease rice tiller number through the transcriptional activation of *OsTB1* (Lu *et al.*, 2013). A previous study demonstrated that IPA1 and SLs seem to work independently to control rice tillering (Luo *et al.*, 2012). However, recent studies indicate that D53 can interact with IPA1 and inhibit the transcriptional activation of IPA1. Furthermore, IPA1 binds to the promoter of *D53*, activates its expression, and plays a critical role in the feedback regulation of SL-induced D53 degradation in bread wheat and rice (Liu *et al.*, 2017; Song *et al.*, 2017). Taken together, the earlier reports suggest that the miR156-SPL module has a complex crosstalk with the SL signaling pathway during tillering.

Switchgrass (*Panicum virgatum* L.) is a C4 perennial tall grass in the Gramineae family and is native to North America. It is a dual-purpose forage and bioenergy crop (Lovell *et al.*, 2021). Tillering is one of the most important agronomic traits that determine the biomass yield of switchgrass. The CRISPR/Cas9-induced mutation of *PvTB1*, one SL signaling pathway gene, can increase the tiller number and biomass yield of switchgrass (Liu *et al.*, 2020). However, few SL biosynthetic or signaling genes in switchgrass have been identified and characterized. In addition, previous studies have demonstrated that overexpression of miR156 in switchgrass can significantly increase aerial axillary bud outgrowth, tiller number, and biomass yield (Chuck *et al.*, 2011; Fu *et al.*, 2012). Downregulation of miR156-targeted *PvSPL4* can elevate the expression of *LAX PANICLE1* (*LAX1*) and *MONOCULM1* (*MOC1*) and therefore increase the tiller number in switchgrass (Gou *et al.*, 2017). Moreover, our previous study found that suppressing of miR156-targeted PvSPL2 activity in switchgrass via the chimeric repressor gene silencing technology increases tiller number and reduces lignin accumulation as well (Wu *et al.*, 2016). However, the direct downstream genes of PvSPL2 that are involved in switchgrass tillering remain largely unknown.

In this study, we found that *PvLBO* was significantly downregulated in the miR156 overexpressing ($miR156_{OE}$) transgenic switchgrass plants, and that overexpression of *PvLBO* in the $miR156_{OE}$ transgenic line can reduce tiller number to even less than that of control switchgrass plants. Based on these results, we propose that *PvLBO* functions in miR156-SPL mediated tillering regulation. Overexpression of *PvLBO* in switchgrass significantly reduced the tiller density, while downregulation of *PvLBO* led to a substantial increase in tiller number. Moreover, we demonstrate for the first time that PvSPL2 was able to bind to the *PvLBO* promoter directly, activate its transcription, and therefore repress switchgrass tillering. Therefore, our results indicate that *PvLBO* acts as a crucial downstream factor in the crosstalk between the SL biosynthetic pathway and the miR156-SPL2 module during the regulation of switchgrass tillering.

Materials and Methods

Plant growth conditions

A lowland-type switchgrass cultivar, Alamo ($2n = 4x = 36$), was employed for genetic transformation and molecular and biochemical analysis. Plants were grown in a glasshouse under a 16-h light photoperiod with supplementary lighting supplied by parabolic aluminized reflector lamps (390 $\mu mol\ m^{-2}\ s^{-1}$).

The temperature in the glasshouse ranged from 25 to 29°C. Plants were watered two times a week and fertilized with Peters $N/P_2O_5/K_2O$-20-10-20 fertilizer (J.R. Peters Inc., Allentown, PA, USA). Primary transgenic plants were propagated by transferring the same numbers of tillers into each pot. Three copies of each line were grown in three-gallon pots. The development of switchgrass in the glasshouse was divided into three vegetative stages (V1, V2 and V3), five elongation stages (E1, E2, E3, E4 and E5) and three reproductive stages (R1, R2 and R3) according to previously outlined method (Hardin *et al.*, 2013). The control and modified plants at E3 stage were trimmed back and then treated with 10 ml of 2 μM *rac*-GR24 and 4 μM TIS108 (Coolaber, Beijing, China) or an equal volume of water every other 2 d. After 35 d, we took photographs and analyzed tiller numbers.

Gene expression quantification

Total RNA was extracted from different tissues and organs of switchgrass and were reverse transcribed into complementary DNA (cDNA) after treatment with genomic DNA (gDNA) Eraser. Total RNAs SYBR Premix ExTaq™ (Takara, Dalian, China) was employed for quantitative real-time polymerase chain reaction (qRT-PCR). Mature miR156 levels were detected and quantified using a highly sensitive qRT-PCR method (Varkonyi-Gasic *et al.*, 2007). The primers used for qRT-PCR are listed in Supporting Information Table S1.

Identification and cloning of *PvLBO*

PvLBO was identified through searching the switchgrass genome database v.4.1 (http://www.phytozome.org/) using the AtLBO sequence (Table S2). Alignment of multiple sequences and phylogenetic tree analysis of PvLBO and its orthologs in *Arabidopsis thaliana*, *Medicago truncatula*, *Populus trichocarpa*, *Oryza sativa* and *Zea mays* were conducted using MEGAX software suite (http://www.megasoftware.net). The full-length sequence cDNA of *PvLBO* was isolated from switchgrass stem by PCR and was subjected to sequencing.

Generation of transgenic switchgrass plants

The overexpressing vectors of pANIC6A-PvLBO and pANIC6D-PvLBO and the RNA interference (RNAi) vector of pANIC8B-PvLBO were constructed as described (Mann *et al.*, 2012). These vectors were individually transformed into *Agrobacterium tumefaciens* strain EHA105. A high-quality embryogenic callus line with a single genotype was established by the large-scale screening of switchgrass Alamo seed-induced calli and was used for *Agrobacterium*-mediated transformation following the procedure described by Xi *et al.* (2009). To produce double transformed switchgrass lines, the calli induced from inflorescences of the selected $TmiR156_{OE\text{-}33}$ transgenic line (Fu *et al.*, 2012) was used to retransform the pANIC6D-PvLBO construct into the miR156 overexpression background.

Transcriptomic analysis

RNA-sequencing (RNA-Seq) was performed using an Illumina Novaseq™ 6000 (LC Sciences, Houston, TX, USA). Transcripts were assembled using HISAT2 software and quantified using STRINGTIE (https://ccb.jhu.edu/software/stringtie/gffcompare.shtml). GFFCOMPARE software was used to construct a comprehensive transcriptome. The differentially expressed genes (DEGs) were selected for gene ontology (GO) enrichment analysis. DEGs from the RNA-Seq data were used for GO category enrichment analysis. Twenty enriched pathways of DEGs were performed.

Determination of carotenoids and chlorophyll contents

The leaf blade and leaf sheath of internode 4 were harvested from transgenic and control switchgrass plants at the E5 stage, and ground in liquid nitrogen. The total contents of carotenoid, chlorophyll *a*, and chlorophyll *b* were examined as described (Sumanta *et al.*, 2014).

Total lignin content analysis

Stems of the control and $PvLBO_{OE}$ transgenic switchgrass plants at the E5 stage were harvested. The resulting samples were ground in liquid nitrogen and lyophilized. Lyophilized extractive-free cell wall residue (CWR) was used for lignin analysis. The AcBr method was employed to quantify total lignin content (Hatfield *et al.*, 1999).

Luciferase (LUC) reporter assay

The vectors of pCAMBIA1300-rPvSPL2 and pCAMBIA1300-rPvSPL4 were transformed into EHA105 and used as effectors. These promoter sequences are listed in Table S3. *PvLBOpro*::LUC, *mPvLBOpro*::LUC, *S1*::LUC, and *S2*::LUC were transformed into the EHA105 cells using the helper plasmid pSoup19. In addition, the *PvD53* promoter, with five GTAC motifs, was amplified by PCR and cloned into the pGreenII 0800-LUC and transformed with pSoup19 as a reporter. The transformed *Agrobacterium* cultures were individually infiltrated into different regions of the same *Nicotiana benthamiana* leaves (Thompson *et al.*, 1991; Hellens *et al.*, 2005). The treated leaves were analyzed for luciferase (LUC) fluorescence activity assay.

Chromatin immunoprecipitation-quantitative polymerase chain reaction (ChIP-qPCR) assay

The ORF sequence of *rPvSPL2* was amplified, fused to an *eGFP* sequence, and cloned into the pANIC6B vector. Transgenic switchgrass lines overexpressing pANIC6B-rPvSPL2-eGFP were selected for chromatin immunoprecipitation quantitative polymerase chain reaction (ChIP-qPCR) assays using the previously described methods (Gendrel *et al.*, 2005). Briefly, 1 g leaf tissue was harvested from each 4-wk-old seedling and ground in liquid nitrogen. The samples were individually crosslinked using 1% (v/v) formaldehyde under the vacuum for 5 min. Chromatin complexes were isolated from individual samples, sonicated for 30 s, 10 times (left on ice for 30 s between each sonication), and then

incubated in an anti-green fluorescent protein (anti-GFP) polyclonal antibody solution (632569; Takara). The recovered DNA from ChIP and 10% input DNA control was then used for qPCR analyses.

Yeast one-hybrid (Y1H) and yeast two-hybrid (Y2H) assays

The full-length cDNAs of *rPvSPL2* and *rPvSPL4* were fused to the pGADT7 (AD) vector respectively. The sequence fragments of *S1* and *S2* described earlier were individually fused to the pHIS2.1 vector. The construct groups were transformed into the yeast strain Y187. The yeast one-hybrid (Y1H) assay was performed according to the manufacturer's instructions.

The full-length *PvSPL2* coding sequence was cloned into the pGBKT7 vector, and the full-length *PvD53* coding sequence was cloned into the pGADT7 vector. Plasmid pGBKT7-PvSPL2 and pGADT7-PvD53 were co-transformed into AH109 yeast cells and screened on the SD/-Leu-Trp medium. The yeast two-hybrid (Y2H) assay was performed according to the manufacturer's instructions.

Electrophoretic mobility shift assay

The full-length cDNAs of *rPvSPL2* and *PvrSPL4* were fused to the pGEX4T-1 expression vector, respectively. The pGEX4T-1-rPvSPL2 construct was transformed into *Escherichia coli Transetta*, and protein expression was induced at 16°C for 12 h with 0.2 mM isopropyl β-D-thiogalactoside (IPTG; Sigma-Aldrich, St Louis, MO, USA). Reactions were performed using a chemiluminescent electrophoretic mobility shift assay (EMSA) kit (Beyotime, Shanghai, China) according to the manufacturer's instructions.

In situ hybridization

The probe sequence of *PvLBO* was amplified by PCR and cloned into the pSPT18 vector. Digoxigenin-labeled sense and antisense probes were synthesized with SP6 and T7 RNA polymerase (Roche, Shanghai, China). The samples of control and transgenic plants were prepared following pre-treatment and hybridization methods as described (Zhang *et al.*, 2007).

Results

PvLBO was downregulated in miR156$_{OE}$ transgenic switchgrass plants

The miR156 and SLs both regulate branching/tillering in various plant species. Our previous results have shown that overexpression of miR156 in switchgrass can significantly increase the number of tillers (Fu *et al.*, 2012). To study the relationship between miR156 and SLs, we treated the wild-type and miR156$_{OE}$ transgenic switchgrass plants with *rac*-GR24, one synthetic SL analog, and TIS108, one SL-biosynthesis inhibitor. As the results exhibited, *rac*-GR24 repressed tillering in both wild-type and miR156$_{OE}$ transgenic plants, implying that the biosynthesis of SLs might be impaired in miR156$_{OE}$ transgenic switchgrass plants (Fig. 1a,b). In contrast, TIS108 only promoted tillering in the wild-type (Fig. 1a,b). It further suggested that overexpression of miR156 in switchgrass might disrupt the function of SL biosynthetic genes acting downstream of *MAX1* since TIS108 has been considered as an efficient inhibitor of MAX1 (Ito *et al.*, 2013). Interestingly, further analysis revealed that the transcripts of one downstream SL biosynthetic gene, *PvLBO* (gene number: *Pavir.5NG619800*) were negatively correlated with the abundances of mature miR156 in the miR156$_{OE}$ transgenic plants (Figs 1c, S1). These results imply that *PvLBO* could play an important role in the miR156-PvSPL module when regulating switchgrass tillering.

To further clarify the functions of *PvLBO*, the coding sequence (CDS) was cloned from lowland-ecotype switchgrass cv Alamo. Other LBOs were then retrieved from maize, rice, *Arabidopsis*, *M. truncatula* and poplar. Phylogenetic analysis showed

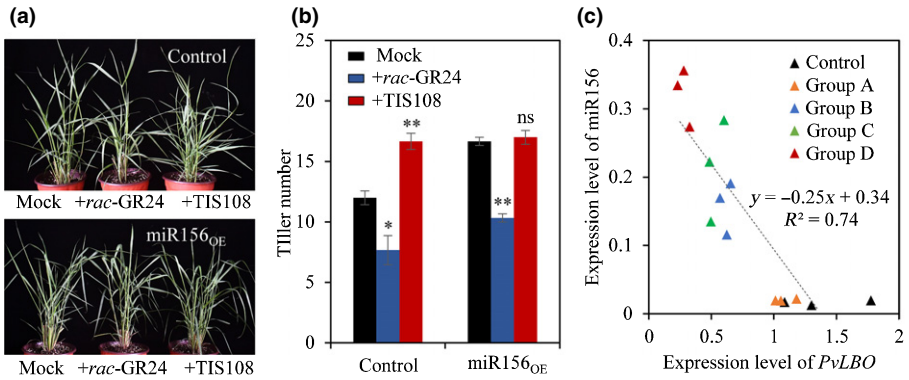

Fig. 1 Overexpression of miR156 compromises strigolactone (SL) synthesis. (a) Gross morphologies of the control and miR156$_{OE}$ transgenic switchgrass plants at the V3 stage with treatment by 2 μM *rac*-GR24 and 4 μM TIS108. (b) Statistical analysis of tiller number of (a). Values are means ± SE ($n = 3$). Student's *t*-test, *, $P < 0.05$; **, $P < 0.01$; ns, no significance. (c) Correlation between miR156 and *PvLBO* expression levels in miR156$_{OE}$ transgenic switchgrass lines. The control and group A transgenic plants had comparable levels of miR156 and exhibited normal growth and tiller number. The levels of miR156 and tiller number were significantly increased in groups B, C and D transgenic plants. Among these miR156$_{OE}$ transgenic lines, relatively low levels of miR156 were observed in group B plants, moderate levels of mature miR156 were found in group C lines, high levels of miR156 were observed in group D.

that PvLBO is clustered together with maize and rice LBO sequences (Fig. 2a). Moreover, alignment of amino acid sequences revealed that PvLBO shared high sequence identity with AtLBO and ZmLBO, and contained the hallmark amino acid residues (i.e. His-250, Asp-252, and His-307) required for iron-binding, and Arg-317 for the interaction with the substrate (red asterisks) in the 2-oxoglutarate and iron(II)-dependent dioxygenases superfamily domain (Fig. 2b). The results of qRT-PCR showed that *PvLBO* was expressed ubiquitously in different switchgrass tissues, and with the highest transcript level in the E2L2 tissue (leaf 2 of switchgrass plants at the E2 stage) followed by the E3L2 tissue (leaf 2 of switchgrass plants at the E3 stage), and then crown buds and roots (Fig. 2c). These findings are consistent with the research into AtLBO, and suggest that PvLBO can also have the ability to oxidize MeCLA to 1′-HO-MeCLA in switchgrass.

To demonstrate the roles of *PvLBO* in the miR156-PvSPL module, we overexpressed *PvLBO* in a miR156$_{OE}$ transgenic switchgrass line (miR156$_{OE\text{-}33}$) that exhibited characteristic morphological changes resulting from miR156 overexpression (Fig. 3a). Among these double transformed switchgrass plants, 27, 4 and 7 lines showed a significant stepped-up increase in *PvLBO* transcripts (Fig. 3b). The tiller numbers were decreased dramatically in the double transformed switchgrass plants compared with miR156$_{OE\text{-}33}$ transgenic plants, and even with the control switchgrass plants (Fig. 3a,c). These results indicated PvLBO is likely a critical downstream effector contributing to the miR156-PvSPL module during the regulation of switchgrass tillering.

PvLBO regulates switchgrass tillering

Then the coding sequence of *PvLBO* driven by *ZmUbi1* promoter was introduced into the wild-type switchgrass by *Agrobacterium*-mediated transformation. Six positive transgenic lines were divided into two groups (i.e. LBO$_{OEI}$ and LBO$_{OEII}$) based on their number of tillers (Figs 4a, S2). The qRT-PCR analysis showed that the LBO$_{OEII}$ plants had much higher expression levels of *PvLBO* and displayed much stronger reductions in tiller number compared with the control plants (Fig. 4b).

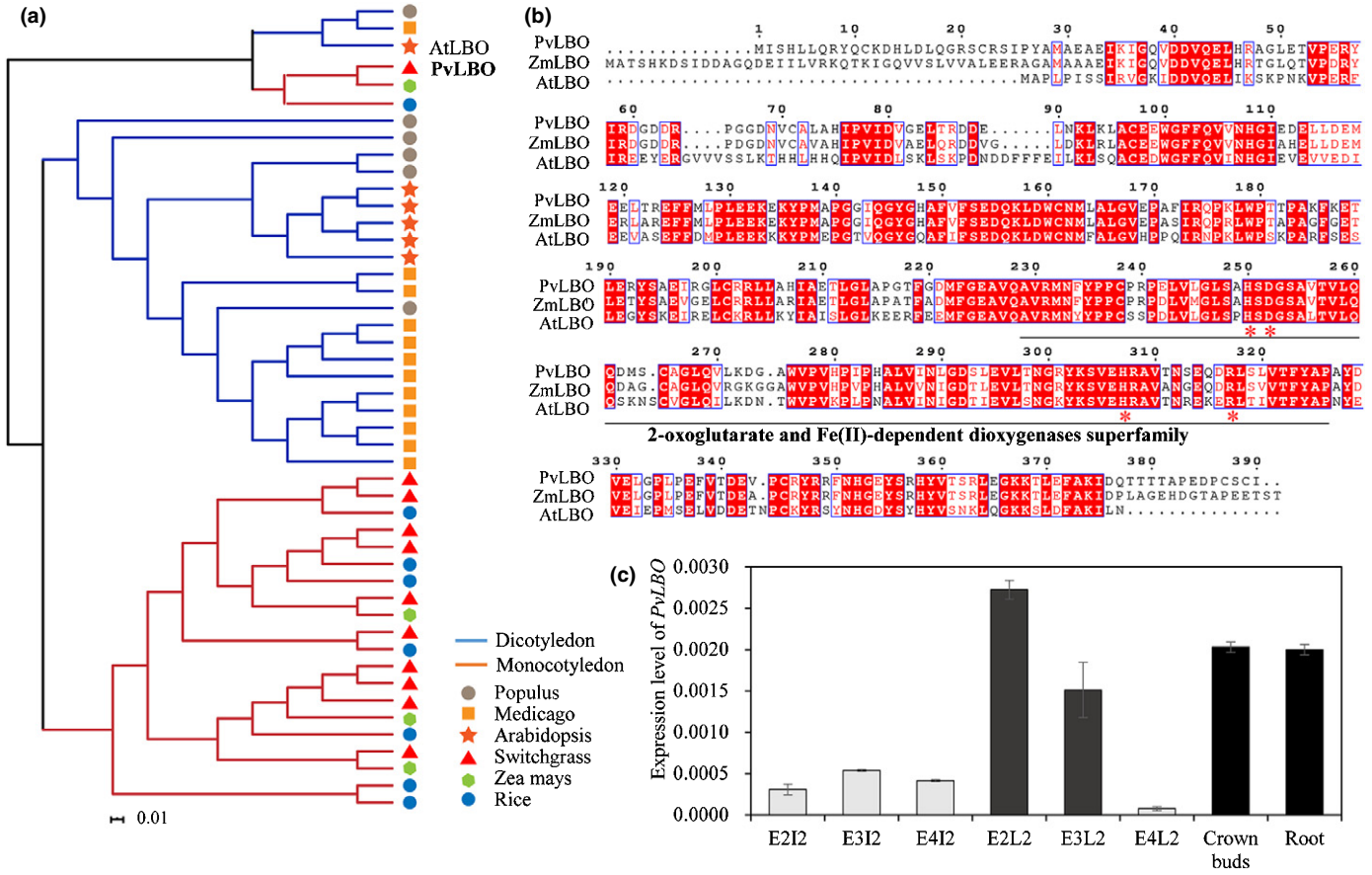

Fig. 2 Phylogenetic analysis, conserved domain alignment and expression pattern of *PvLBO*. (a) A phylogenetic tree showing the relationship between PvLBO and the LBOs from different plant species. The phylogenetic tree was constructed based on the alignment using the MEGAX software. (b) Protein sequences alignment shows the differences among the AtLBO (AT3G21420), PvLBO and ZmLBO. (c) Expression levels of *PvLBO* in crown buds, root, internodes, and leaves of the wild-type switchgrass. The quantitative real-time polymerase chain reaction (qRT-PCR) data were normalized against the expression level of switchgrass *PvUbq2*. The values are the means ± SE ($n = 3$). E2I2, internode 2 of the stem elongation 2 stage; E3I2, internode 2 of the stem elongation 3 stage; E4I2, internode 2 of the stem elongation 4 stage; E3L2, leaf 2 of the stem elongation 3 stage; E4L2, leaf 2 of the stem elongation 4 stage. Crown buds and roots were collected from the wild-type switchgrass at the E4 stage.

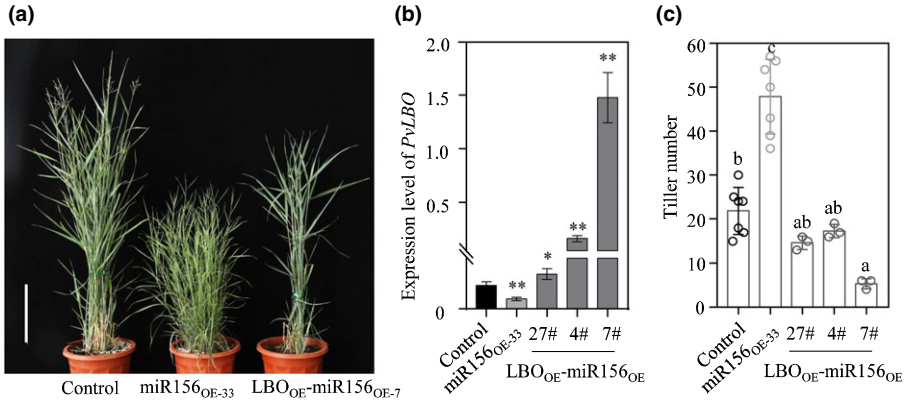

Fig. 3 Overexpression of *PvLBO* reduced the increased tillering in miR156 overexpressing switchgrass. (a) Overexpression of *PvLBO* in the miR156$_{OE-33}$ transgenic plants reduced the tiller number. Bar, 20 cm. (b) The expression levels of *PvLBO* were determined through quantitative real-time polymerase chain reaction (qRT-PCR). The expression level of *PvUbq2* was used as an internal control. Values are means ± SE ($n = 3$). Student's *t*-test, *, $P < 0.05$; **, $P < 0.01$. (c) Statistical analysis of tiller numbers of the control, miR156$_{OE-33}$ and LBO$_{OE}$-miR156$_{OE}$ transgenic switchgrass plants at the reproductive two stage of the control plants. Values are means ± SE ($n = 3$–7). The letters above the error bars indicate significant differences determined by one-way ANOVA ($P < 0.05$, Duncan's multiple-range test). Control plants were produced with pANIC6B empty vector from the same experimental batch.

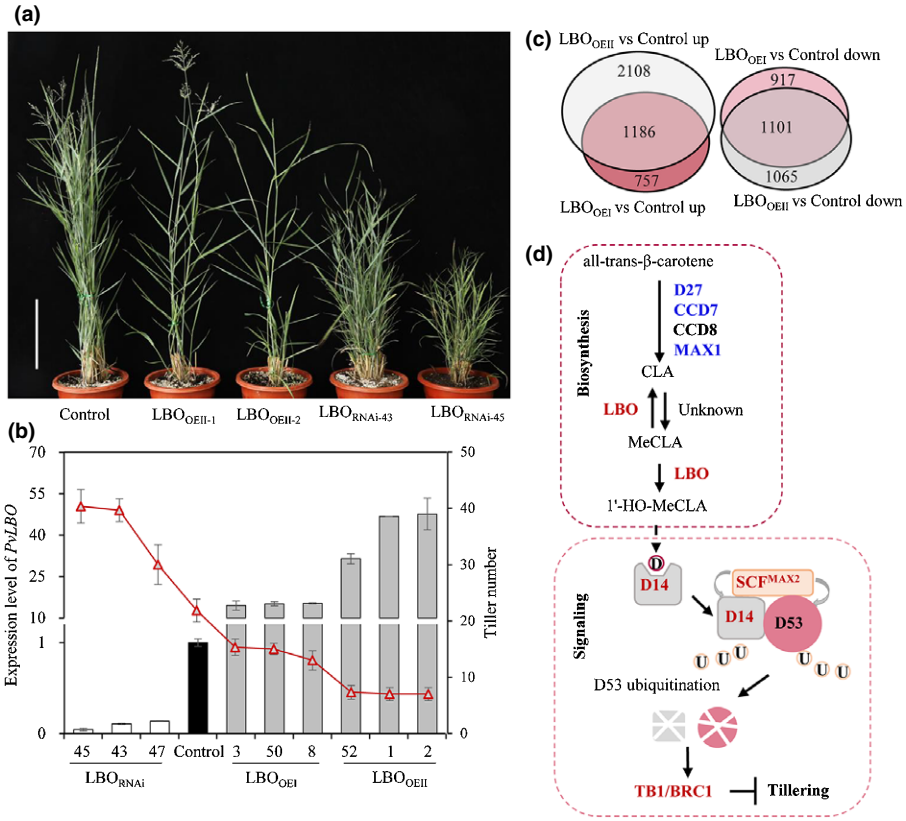

Fig. 4 PvLBO regulated tillering of switchgrass. (a) Phenotypic characterizations of the control, LBO$_{OEII}$ and LBO$_{RNAi}$ transgenic switchgrass plants at the reproductive two stage of control plants. Bar, 20 cm. (b) The expression levels of *PvLBO* and tiller numbers of control and transgenic plants at the E4 stage. The expression levels of *PvLBO* were determined through quantitative real-time polymerase chain reaction (qRT-PCR). The expression level of *PvUbq2* was used as an internal control. Values are means ± SE ($n = 3$). The columns represent the expression levels of *PvLBO*. The red triangular markers represent tiller numbers. (c) Overview of upregulated and downregulated genes in the control and LBO$_{OE}$ transgenic plants, determined through RNA-sequencing. The numbers represent the altered genes in various samples. The numbers in the overlapped areas represent the genes observed in both libraries. (d) A diagram showing both strigolactone (SL) biosynthesis and signaling pathways. Blue letters mean that genes were downregulated in the transgenic plants compared to the control plants, while the red letters mean that genes were upregulated. The blunt ended arrow means tillering inhibition. Control plants were produced with the empty vector from the same experimental batch.

Additionally, the stems of the LBO_{OEII} plants were thicker, the node numbers of LBO_{OEII} plants were increased, and the leaves were wider and longer compared with the control plants (Fig. S3). Moreover, we found that the tiller number of each plant was negatively correlated with the expression level of *PvLBO* (Fig. 4b). Alternatively, the expression levels of the SL-responsive gene, *PvTB1*, were significantly upregulated in the LBO_{OEI} and LBO_{OEII} plants (Fig. S4a). This finding indicates that PvLBO is likely a key enzyme of the SL biosynthetic pathway and plays a vital role in regulating the tillering of switchgrass.

To further investigate the function of *PvLBO*, we generated *PvLBO* downregulation transgenic switchgrass lines using RNAi technology. As expected, the LBO_{RNAi} transgenic lines exhibited higher tiller numbers but semidwarf phenotypes with shorter internodes (Fig. 4a,b). It is noteworthy that downregulation of *PvLBO* promoted the elongation of axillary buds and produced axillary shoots at some nodes (Fig. S5). In addition, we treated LBO_{RNAi} and LBO_{OE} transgenic switchgrass plants with *rac*-GR24 and TIS108, respectively. As anticipated, the tiller number was significantly reduced in the LBO_{RNAi} plants after treatment with 2 μM *rac*-GR24, whereas more tillers formed from the LBO_{OE} transgenic plants after treatment with 4 μM TIS108 (Fig. S6). The treatment results specifically support a role for *PvLBO* in SL biosynthesis, downstream of TIS108 inhibition.

Numerous genes were changed in PvLBO$_{OE}$ transgenic switchgrass plants

To assess the global effects of *PvLBO* overexpression on SL biosynthesis, signaling pathways, and responses, we extracted RNA from the stems of the representative LBO_{OEI} and LBO_{OEII} transgenic lines and performed transcriptome analysis by high-throughput RNA-Seq. RNA-Seq data revealed a total of 1943 genes were significantly upregulated, and 2018 genes were significantly downregulated in the LBO_{OEI} plants compared to the control plants. In the LBO_{OEII} plants, 3294 genes were significantly upregulated and 2166 genes were significantly downregulated compared to the control plants (Fig. 4c; Tables S4, S5). Previous studies in *Arabidopsis* and poplar have shown that the SL biosynthetic genes are involved in the negative feedback on the SL biosynthesis (Mashiguchi *et al.*, 2009), whereas the SL perception and signaling genes participate in the positive feedback (Katyayini *et al.*, 2019). We also found that the SL biosynthetic genes, such as *PvD27*, *PvCCD7* and *PvMAX1* were downregulated in the LBO_{OEI} and LBO_{OEII} transgenic plants (Fig. 4d; Table S6). As expected, the SL perception and signaling genes, *PvD14* and *PvMAX2*, were upregulated in the LBO_{OEI} and LBO_{OEII} transgenic plants (Fig. 4d; Table S6), suggesting that more bioactive SL compounds were synthesized in the LBO_{OE} transgenic switchgrass. This result was confirmed by qRT-PCR (Fig. S4b). Furthermore, GO category enrichment analysis of DEGs showed that plant hormone signal transduction was the most enriched item in the biological process. Other processes such as response to karrikin, lignin catabolism, salicylic acid catabolism, and regulation of phenylpropanoid metabolism were also enriched (Fig. S7). These results demonstrate that *PvLBO* is an effective gene involved in SL biosynthesis in switchgrass.

PvLBO affected carotenoid, chlorophyll, and lignin biosynthesis in switchgrass

Strigolactones are a group of isoprenoid-based phytohormones derived from carotenoids. In this study, the total carotenoid content decreased by 25–40% in the LBO_{OEI} and LBO_{OEII} plants compared with the control plants (Fig. S8). Therefore, the rate of SL biosynthesis could be promoted as the concentration of substrate increases in the overexpression transgenic switchgrass plants. Additionally, the contents of Chl*a* and Chl*b*, which share the geranylgeranyl pyrophosphate precursor with carotenoids, were significantly decreased in the LBO_{OEI} and LBO_{OEII} plants, while Chl*a* was accumulated in LBO_{RNAi} plants (Fig. S8). Most surprisingly, the transcriptome analysis showed that numerous genes involved in the lignin biosynthetic pathway, as well as the transcriptional activator *PvMYB103*, *PvMYB42*, *PvMYB61*, and *PvMYB63*, were downregulated in LBO_{OE} transgenic switchgrass plants (Fig. S9). In contrast, the expression levels of the transcriptional suppressor *PvMYB4* were upregulated in the LBO_{OE} plants (Fig. S9b). Based on the results, we hypothesized that overexpression of *PvLBO* in switchgrass could affect lignin biosynthesis. The content of acid-insoluble lignin in the LBO_{OE} plants decreased by approximately 33% compared with the control plants (Fig. S10). In contrast, the contents of acid-insoluble lignin were increased in the LBO_{RNAi} transgenic switchgrass plants (Fig. S10). Taken together, these findings suggest that SLs could regulate lignin biosynthesis of stems in switchgrass.

PvSPL2 directly bound to the *PvLBO* promoter directly and activated its transcription in switchgrass

Our previous study has shown that miR156-targeted PvSPL2 plays an essential role in switchgrass tillering (Wu *et al.*, 2016). Expression profiles of *PvSPL2* and *PvLBO* in various tissues and phases of switchgrass revealed an appreciable co-expression between *PvSPL2* and *PvLBO* in the tissues of the roots, crown and nodes at the E4 stage (Fig. 5a). It suggests that PvSPL2 has the potential to regulate *PvLBO* expression temporally and spatially. Furthermore, we found there are two SBP binding motifs (GTAC) in a 1397 bp upstream sequence of the *PvLBO* promoter (Fig. 5b). Dual-LUC reporter assays showed that *35S::rPvSPL2* and *PvLBOpro::LUC* co-infiltrating significantly increased the luminescence intensity, while *35S::rPvSPL2* and mutated *mPvLBOpro::LUC* co-infiltrating had even lower luminescence intensity than the negative control (Fig. 5c,d), suggesting that PvSPL2 can bind to the motif of the *PvLBO* promoter and activate its transcription. Furthermore, ChIP-qPCR analysis of PvSPL2-GFP revealed an apparent enrichment of site 2 in the *PvLBO* promoter (Fig. 5e). About 200 bp regions of *PvLBO* promoter containing sites 1 and 2 (referred to as S1 and S2), respectively, were used for further identification of the core motif recognized by PvSPL2. The LUC reporter assays and Y1H showed that site 2 was necessary and sufficient for PvSPL2-responsive transcription (Fig. 5f,g). Moreover, EMSA showed that PvSPL2 bound to probe 1 and probe 2 (44 bp length

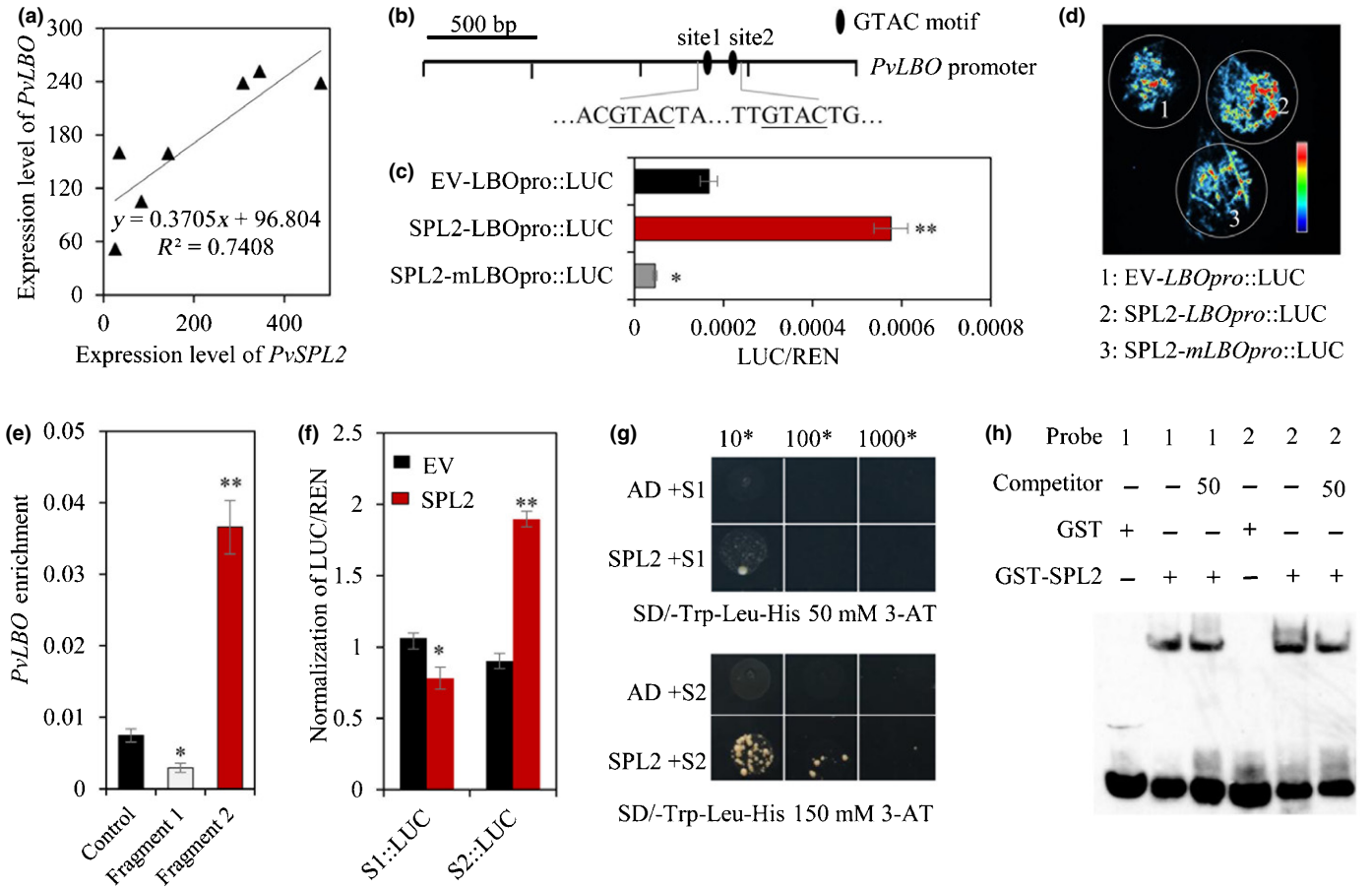

Fig. 5 *PvLBO*expression was activated by PvSPL2 in switchgrass. (a) Correlations between expression levels of *PvSPL2* and *PvLBO* in different tissues and organs of switchgrass. The representative probe sets of *PvSPL2* (AP13CTG29191_at) and *PvLBO* (AP13ITG40875_at) were retrieved from the switchgrass gene expression atlas. (b) Schematic presentation of putative SPL binding sites in the *PvLBO* promoter. (c) Dual-luciferase (LUC) reporter assay showing the activation of *PvLBO* expression by the PvSPL2 effector compared to the control effector. *mLBOpro*::LUC shows that two GTAC motifs in *PvLBO* promoters were mutated to ACGT. The empty vector pCAMBIA 1300 (EV) was employed as the control effector. Values are means ± SE ($n = 3$). Student's *t*-test, *, $P < 0.05$; **, $P < 0.01$. (d) Image of the LUC reporter assay presenting the fluorescence intensity, 1, pCAMBIA1300 and *LBOpro*::LUC; 2, SPL2 and *LBOpro*::LUC; 3, SPL2 and *mLBOpro*::LUC. (e) Chromatin immunoprecipitation-quantitative polymerase chain reaction (ChIP-qPCR) analysis of *rPvSPL2-GFP* overexpressing transgenic switchgrass. Crude chromatin extracts were immunoprecipitated with anti-green fluorescent protein (anti-GFP) antibodies. Purified ChIP and input DNAs were used for qPCR analyses. *rPvSPL2*, miR156-resistant *PvSPL2*. Values are means ± SE ($n = 3$). Student's *t*-test, *, $P < 0.05$; **, $P < 0.01$. (f) The normalization of the LUC : REN ratio in the LUC assay indicates relative luciferase activity of different fragmenst in the *PvLBO* promoter. The empty vector pCAMBIA 1300 (EV) was used as the control effector. Values are means ± SE ($n = 3$). Student's *t*-test, *, $P < 0.05$; **, $P < 0.01$. (g) Growth of yeast cells on SD/-Trp-Leu-His supplemented with 3-AT. pHIS2.1-*ProS1* plus pGADT7 (50 mM 3-AT) and pHIS2.1-*ProS2* plus pGADT7 (150 mM 3-AT) served as the negative controls. (h) Electrophoretic mobility shift assay (EMSA) showing PvSPL2 binding to its target sequence in *PvLBO* promoter. Panel 1 shows that the GST tag does not bind to the biotin-labeled probe 1; panel 2 shows that PvSPL2 binds to its target probe 1, and panel 3 shows competition of binding by the unlabeled probe 1. Panel 4 shows that the GST tag does not bind to the biotin-labeled probe 2; panel 5 shows that PvSPL2 binds to its target probe 2, and panel 6 shows competition of binding by the unlabeled probe 2.

sequence around site 1 and site 2) *in vitro* (Fig. 5h). These results revealed that PvSPL2 was an efficient transcriptional activator of *PvLBO*, suggesting the presence of putative crosstalk between the SL biosynthesis and miR156-SPL module during switchgrass tillering regulation.

PvLBO and SL signaling genes were upregulated in *PvSPL2* overexpressing transgenic switchgrass plants

To confirm the regulation of *PvLBO* by PvSPL2 *in vivo* and the spatial expression pattern of *PvLBO* in the control, $SPL2_{OE}$ and $miR156_{OE}$ transgenic switchgrass plants were performed by *in situ* hybridization (Fig. 6a,b). The *PvLBO* gene was preferentially expressed on the apex of the shoot apical and floral meristems of control switchgrass plants. Furthermore, *in situ* hybridization analysis revealed that more *PvLBO* transcripts accumulated in $SPL2_{OE}$ plants. In contrast, the transcript abundance of *PvLBO* was obviously reduced in $miR156_{OE}$ plants (Fig. 6a,b). Moreover, the results of the qRT-PCR showed that the expression level of *PvLBO* as well as three SL signaling genes, *PvMAX2*, *PvD14*, and *PvTB1* were consistently upregulated in all $SPL2_{OE}$ transgenic lines analyzed by this study (Figs 6c, S11).

Additionally, our Y1H and LUC reporter assay also suggested that PvSPL4 could bind to the *PvLBO* promoter and then

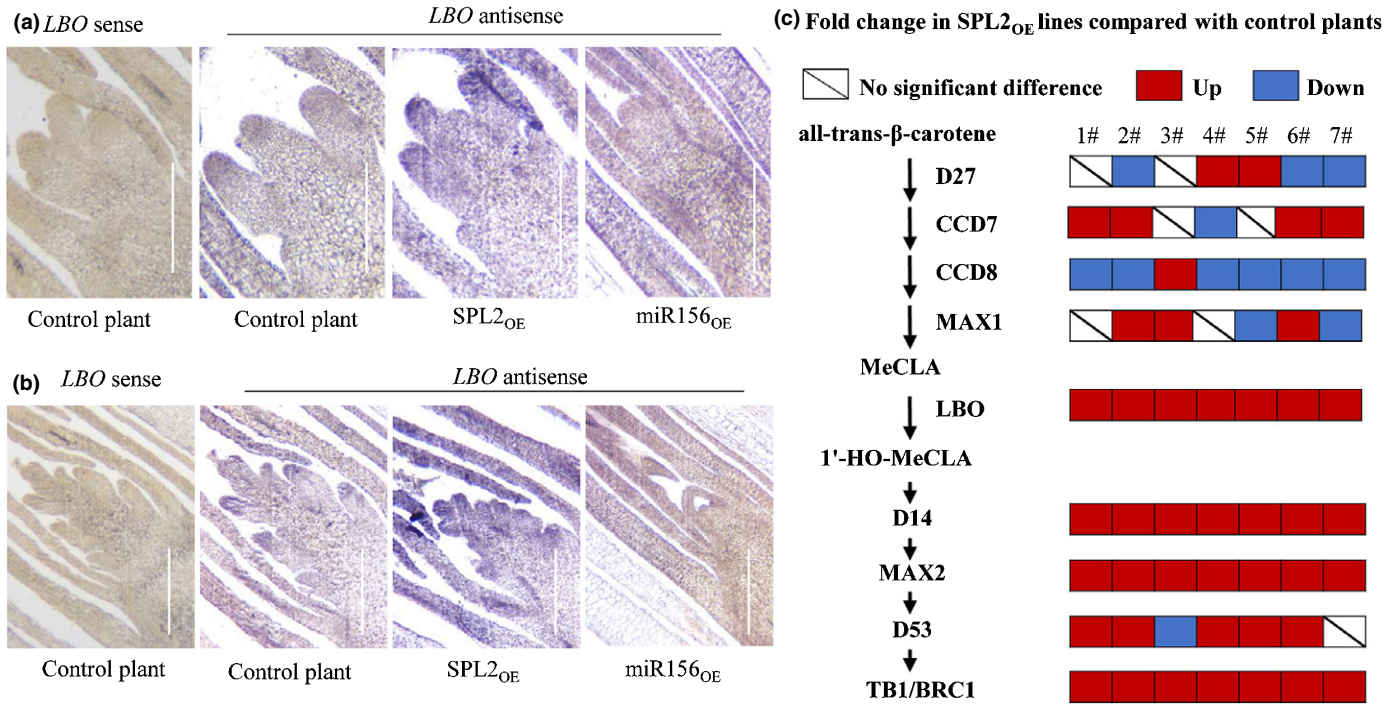

Fig. 6 Expression levels of strigolactone (SL) biosynthetic and signaling genes among in $SPL2_{OE}$ transgenic switchgrass compared to control plants. RNA *in situ* hybridization of *PvLBO* with antisense probes in shoot apical (a) and floral (b) meristems of the control, $SPL2_{OE}$, and $miR156_{OE}$ transgenic switchgrass plants. Bar, 200 μm. (c) The expression level of *PvUbq2* was used as an internal control. Values are means ± SE ($n = 3$). Significant differences were determined using Student's *t*-test, $P < 0.05$. Oblique line square shows there were no significant difference between the control and $SPL2_{OE}$ transgenic switchgrass plants, 1# to 7# means seven individual $SPL2_{OE}$ transgenic lines. The blue square means that genes were downregulated, while the red square means that genes were upregulated in the $SPL2_{OE}$ transgenic switchgrass plants. Control plants were produced with pANIC6B empty vector from the same experimental batch.

activate its transcription as well. However, there are irregular changes in the expression levels of *PvLBO* in $SPL4_{OE}$ transgenic switchgrass plants, indicating that there is a complicated relationship between PvSPL4 and *PvLBO* (Fig. S12). In addition, Y2H analysis and LUC reporter assay revealed that PvSPL2 can interact with PvD53 (Fig. S13). Altogether, our results suggest that *PvLBO* is a novel target gene of PvSPL2 and functions in the crosstalk between the SL biosynthetic pathway and the miR156-SPL2 module in switchgrass (Fig. 7).

Discussion

The noncanonical SL biosynthetic gene *LBO* is present in many seed plant species and acts in the later steps after CLA synthesis (Yoneyama *et al.*, 2020). It is a novel branching-associated gene originally identified in *Arabidopsis* (Brewer *et al.*, 2016). The LBOs from *Arabidopsis*, tomato, maize, and sorghum can convert MeCLA to 1′-HO-MeCLA *in vitro* (Yoneyama *et al.*, 2020). Metabolite analysis has suggested that noncanonical SLs are likely predominant in *Arabidopsis* (Brewer *et al.*, 2016). The biosynthesis of SLs has been widely studied in rice as well (Mashiguchi *et al.*, 2021). However, in contrast to *Arabidopsis*, the canonical SL 4DO is a major endogenous inhibitor of tillering in rice (Mashiguchi *et al.*, 2021). Thus, the function of LBO in monocots is still elusive. Switchgrass is an important perennial monocotyledonous grass, which is used to produce fodder and biofuels (Lovell *et al.*, 2021). Previous studies have demonstrated that the miR156-SPL module can control switchgrass tillering (Chuck *et al.*, 2011; Fu *et al.*, 2012; Wu *et al.*, 2016; Gou *et al.*, 2017). Similar observations have been reported in maize and rice (Xie *et al.*, 2006; Chuck *et al.*, 2007). In this study, we found that *PvLBO* plays an important role in the control of switchgrass tillering. The upregulation of *PvLBO* in switchgrass dramatically inhibited tiller bud outgrowth, while the downregulation of *PvLBO* led to substantial increase in the tiller number. The 1′-HO-MeCLA and its derivatives converted by LBO are highly unstable and hard to detect in plants (Yoneyama *et al.*, 2020). However, the expression levels of SL-responsive genes, *MAX2*, *TCP14a*, and *TB1*, were significantly induced when *PvLBO* were overexpressed, whereas the SL biosynthetic genes, *CCD7* and *MAX1*, were repressed due to the feedback loop of SL biosynthesis. These findings indicate that *PvLBO* could participate in the biosynthesis of active SLs and regulate switchgrass tillering.

Identification and characterization of the transcription factors regulating *LBO* expression are crucial for deciphering the SL biosynthesis in plants. Our previous studies have shown that overexpression of miR156 or *PvSPL2SRDX* in switchgrass can result in drastic increase of tiller number (Fu *et al.*, 2012; Wu *et al.*, 2016). Moreover, the miR156-targeted SPL4 can repress the initiation of aerial axillary buds and tillering as well (Gou *et al.*, 2017). However, the molecular mechanism of switchgrass tillering remains largely unknown, especially in the miR156-SPL

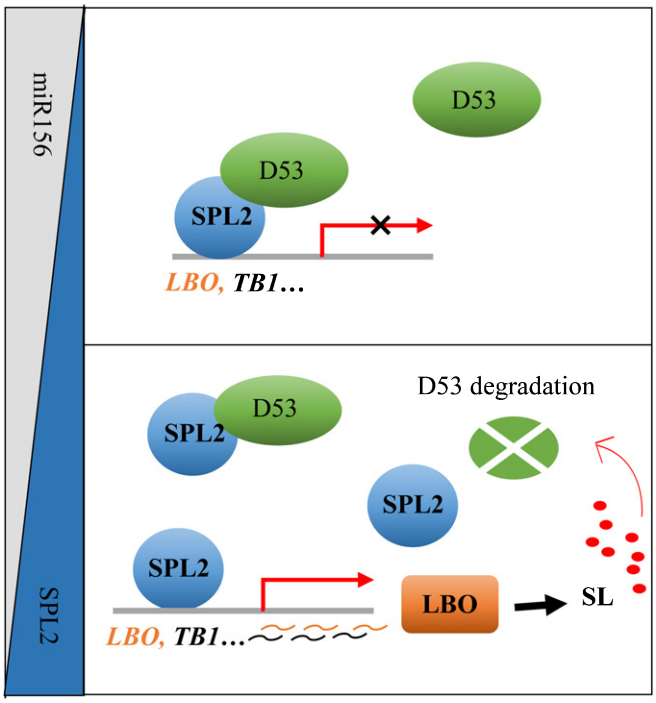

Fig. 7 A proposed tillering regulation model mediated by strigolactones (SLs) and miR156-SPL module in switchgrass. In the presence of miR156, *SPL2* transcripts are cleaved by miR156, while D53 interacts with SPL2 which further inhibits the transcriptional activation of SPL2 to downstream genes, such as *PvTB1* and *PvLBO*. When miR156 levels decreased, the increased PvSPL2 can directly bind to the promoter of *LBO* to activate its expression, and then produce more bioactive SLs. The increased SLs trigger the ubiquitin-mediated degradation of D53. Therefore, more PvSPL2 is released to activate the expressions of downstream genes involved in tillering.

module. In this study, we found that the miR156-targeted PvSPL2 directly bound to the promoter of *PvLBO* and activated its transcription in switchgrass. Therefore, it is reasonable to propose that the miR156-PvSPL2 module is involved in controlling the noncanonical SL synthesis through the transcriptional regulation of *PvLBO* in switchgrass. In addition, the miR156-targeted SPL is a downstream component of D53 in the SL signaling pathway (Liu *et al.*, 2017; Song *et al.*, 2017). Previous study suggests that D53 acts with IPA1 and represses its transcriptional activity by recruiting the TPL–TPR complex in rice. Meanwhile, IPA1 can activate *D53* expression by directly binding to the promoter of *D53*. The feedback regulation between IPA1 and D53 could guarantee the precise regulation of SLs on tiller bud outgrowth in rice (Lovell *et al.*, 2021). However, the miR156 targeted SPLs play a vital role in many crucial biological processes, including tillering, vegetative-to-reproductive phase transition, and flowering. Therefore, an extra mechanism is required to remove or alleviate D53 inhibition in plants. Based on our model, PvSPL2 could lead to the D53 ubiquitin degradation via the transcriptional regulation of SL biosynthesis and therefore remove and/or alleviate D53 inhibition in switchgrass. The released PvSPL2 will promote the transcriptional activation of its downstream genes, including *PvTB1*, which efficiently inhibits tiller bud outgrowth (Fig. 7). Previous study has demonstrated the switchgrass miR156-targeted *SPL4*, one ortholog to rice IPA1, is also involved in tillering (Gou *et al.*, 2017). Our Y1H and LUC reporter assay indicate that PvSPL4 also has potential to activate the expression of *PvLBO*. Unfortunately, no consistent changes were detected in the expression levels of *PvLBO* and *PvSPL4* in the $SPL4_{OE}$ transgenic switchgrass lines, implying a complex network of regulatory interactions between PvSPL4 and *PvLBO*. Additionally, PvSPL2 and PvSPL4 belong to different subfamilies of which the SPL members exhibit functional redundancy and diversity (Wu *et al.*, 2016; Gou *et al.*, 2017). Moreover, PvSPL4 regulates the expression of *LAX* and *MOC1* rather than *TB1* in switchgrass (Gou *et al.*, 2017). Previous studies found that *MOC1* is a critical component required for tillering (Li *et al.*, 2003). Therefore, we suspect that PvSPL2 and PvSPL4 play different roles in switchgrass tillering regulation.

GR24 is a synthetic analog of SLs and its activity triggers SL signaling in plants. The tiller number of $miR156_{OE}$ transgenic switchgrass plants significantly decreased after treatment with a moderate level (2 μM) of *rac*-GR24. Our results are consistent with the observation in the miR156 overexpressing transgenic rice plants treated with high concentrations (10 μM) of *rac*-GR24 (Luo *et al.*, 2012). In contrast, Song *et al.* (2017) found that low levels (1 μM) of *rac*-GR24 slightly inhibited tiller bud outgrowth in the miR156 overexpressing transgenic rice plants. These results suggest that the inhibition of SLs on tiller bud outgrowth in plants is a dosage dependent. In rice, the miR156-SPL engages in crosstalk with the SL signaling pathway through the interaction between D53 and IPA1. Exogenous application of *rac*-GR24 degrades D53 and releases more upregulated IPA1 (Song *et al.*, 2017). D53 and PvSPL2 also interacted in switchgrass, implying a similar mechanism responsible for tillering regulation in switchgrass. However, our results further indicate that the dramatically increased tiller number of miR156 overexpressing transgenic switchgrass plants was due to both a decreased expression of miR156-targeted *PvSPL2* and impaired biosynthesis of SLs. Thus, we believe that PvSPL2 is not only the common target of miR156 and the SL signaling pathway, but also functions as a crucial regulator that fine-tunes the biosynthesis of SLs in switchgrass. However, due to the structural diversity of SLs, the further studies are required to confirm whether the SPL-LBO module exists in other plant species.

Tillering is an important agronomic trait affecting the biomass yield of forage and bioenergy grasses. Both SLs and the miR156-SPL module are involved in the regulation of tiller number in monocot grass species. Our results demonstrate that PvLBO is a crucial enzyme in the noncanonical SL biosynthetic pathway and strongly affected switchgrass tillering. Moreover, *PvLBO* was identified as a novel downstream gene of PvSPL2 in miR156-SPL mediated tillering in switchgrass. Further studies such as SL measurements, SL precursor feeding assays, and heterologous enzyme assays are required to confirm the function of PvLBO in future. However, our study facilitates a better understanding of the regulatory mechanism of grass tillering mediated by SLs and the miR156-SPL module. It will provide novel targets for

improving plant architecture and biomass yield of forage and bioenergy crops through molecular breeding.

Acknowledgements

The authors thank Prof. C. Neal Stewart Jr for providing the pANIC vectors, Dr Xinshun Ding, Prof. Chuanxiao Xie and Prof. Wen-Xue Li for critical reading and discussion of the manuscript. This work was supported by the Agricultural Variety Improvement Project of Shandong Province (no. 2019LZGC010), the National Natural Science Foundation of China (nos. 31672479, 31872879, and 31801429), the Strategic Priority Research Program of the Chinese Academy of Sciences (XDA26030301), and QIBEBT and Dalian National Laboratory for Clean Energy (DNL), CAS (Grant: QIBEBT I201930).

Author contributions

CF, WL and RY designed the research; RY, WL, YS, ZS, ZW, YW and MW performed the experiments; CF, WL, RY, HW and SB analyzed the data; CF, WL and RY wrote the manuscript. RY and WL contributed equally to this work.

ORCID

Chunxiang Fu https://orcid.org/0000-0003-2378-5122

Data availability

Sequence data from this article can be downloaded from the Phytozome database (https://phytozome-next.jgi.doe.gov/). The data that support the findings of this study are available from the corresponding author upon reasonable request.

References

Akiyama K, Matsuzaki K, Hayashi H. 2005. Plant sesquiterpenes induce hyphal branching in arbuscular mycorrhizal fungi. *Nature* **435**: 824–827.

Booker J, Sieberer T, Wright W, Williamson L, Willett B, Stirnberg P, Turnbull C, Srinivasan M, Goddard P, Leyser O. 2005. *MAX1* encodes a cytochrome P450 family member that acts downstream of *MAX3/4* to produce a carotenoid-derived branch-inhibiting hormone. *Developmental Cell* **8**: 443–449.

Braun N, de Saint Germain A, Pillot J-P, Boutet-Mercey S, Dalmais M, Antoniadi I, Li X, Maia-Grondard A, Le Signor C, Bouteiller N *et al.* 2012. The pea TCP transcription factor *PsBRC1* acts downstream of strigolactones to control shoot branching. *Plant Physiology* **158**: 225–238.

Brewer PB, Yoneyama K, Filardo F, Meyers E, Scaffidi A, Frickey T, Akiyama K, Seto Y, Dun EA, Cremer JE *et al.* 2016. *LATERAL BRANCHING OXIDOREDUCTASE* acts in the final stages of strigolactone biosynthesis in *Arabidopsis*. *Proceedings of the National Academy of Sciences, USA* **113**: 6301–6306.

Chevalier F, Nieminen K, Sánchez-Ferrero JC, Rodríguez ML, Chagoyen M, Hardtke CS, Cubas P. 2014. Strigolactone promotes degradation of DWARF14, an α/β hydrolase essential for strigolactone signaling in *Arabidopsis*. *Plant Cell* **26**: 1134–1150.

Chuck G, Cigan AM, Saeteurn K, Hake S. 2007. The heterochronic maize mutant *Corngrass1* results from overexpression of a tandem microRNA. *Nature Genetics* **39**: 544–549.

Chuck GS, Tobias C, Sun L, Kraemer F, Li C, Dibble D, Arora R, Bragg JN, Vogel JP, Singh S *et al.* 2011. Overexpression of the maize *Corngrass1* microRNA prevents flowering, improves digestibility, and increases starch content of switchgrass. *Proceedings of the National Academy of Sciences, USA* **108**: 17550–17555.

Cook CE, Whichard LP, Turner B, Wall ME, Egley GH. 1966. Germination of witchweed (*Striga lutea* Lour.): isolation and properties of a potent stimulant. *Science* **154**: 1189–1190.

Duan J, Yu H, Yuan K, Liao Z, Meng X, Jing Y, Liu G, Chu J, Li J. 2019. Strigolactone promotes cytokinin degradation through transcriptional activation of *CYTOKININ OXIDASE/DEHYDROGENASE 9* in rice. *Proceedings of the National Academy of Sciences, USA* **116**: 14319–14324.

Fu C, Sunkar R, Zhou C, Shen H, Zhang JY, Matts J, Wolf J, Mann DG, Stewart CN Jr., Tang Y *et al.* 2012. Overexpression of miR156 in switchgrass (*Panicum virgatum* L.) results in various morphological alterations and leads to improved biomass production. *Plant Biotechnology Journal* **10**: 443–452.

Gendrel AV, Lippman Z, Martienssen R, Colot V. 2005. Profiling histone modification patterns in plants using genomic tiling microarrays. *Nature Methods* **2**: 213–218.

Gomez-Roldan V, Fermas S, Brewer PB, Puech-Pagès V, Dun EA, Pillot J-P, Letisse F, Matusova R, Danoun S, Portais J-C *et al.* 2008. Strigolactone inhibition of shoot branching. *Nature* **455**: 189–194.

Gou JY, Felippes FF, Liu CJ, Weigel D, Wang JW. 2011. Negative regulation of anthocyanin biosynthesis in *Arabidopsis* by a miR156-targeted SPL transcription factor. *Plant Cell* **23**: 1512–1522.

Gou J, Fu C, Liu S, Tang C, Debnath S, Flanagan A, Ge Y, Tang Y, Jiang Q, Larson PR *et al.* 2017. The miR156-SPL4 module predominantly regulates aerial axillary bud formation and controls shoot architecture. *The New Phytologist* **216**: 829–840.

Hardin CF, Fu C, Hisano H, Xiao X, Shen H, Stewart CN Jr., Parrott W, Dixon R, Wang Z-Y. 2013. Standardization of switchgrass sample collection for cell wall and biomass trait analysis. *BioEnergy Research* **6**: 755–762.

Hatfield RD, Grabber J, Ralph J, Brei K. 1999. Using the acetyl bromide assay to determine lignin concentrations in herbaceous plants: some cautionary notes. *Journal of Agricultural and Food Chemistry* **47**: 628–632.

Hellens RP, Allan AC, Friel EN, Bolitho K, Grafton K, Templeton MD, Karunairetnam S, Gleave AP, Laing WA. 2005. Transient expression vectors for functional genomics, quantification of promoter activity and RNA silencing in plants. *Plant Methods* **1**: 13.

Ito S, Umehara M, Hanada A, Yamaguchi S, Asami T. 2013. Effects of strigolactone-biosynthesis inhibitor TIS108 on *Arabidopsis*. *Plant Signaling & Behavior* **8**: e24193.

Katyayini NU, Rinne P, van der Schoot C. 2019. Strigolactone-based node-to-bud signaling may restrain shoot branching in hybrid aspen. *Plant & Cell Physiology* **60**: 2797–2811.

Li X, Qian Q, Fu Z, Wang Y, Xiong G, Zeng D, Wang X, Liu X, Teng S, Hiroshi F *et al.* 2003. Control of tillering in rice. *Nature* **422**: 618–621.

Liu J, Cheng X, Liu P, Sun J. 2017. miR156-targeted SBP-box transcription factors interact with DWARF53 to regulate *TEOSINTE BRANCHED1* and *BARREN STALK1* expression in bread wheat. *Plant Physiology* **174**: 1931–1948.

Liu Y, Wang W, Yang B, Currey C, Fei SZ. 2020. Functional analysis of the teosinte branched 1 gene in the tetraploid switchgrass (*Panicum virgatum* L.) by CRISPR/Cas9-directed mutagenesis. *Frontiers in Plant Science* **11**: 572193.

Lovell JT, MacQueen AH, Mamidi S, Bonnette J, Jenkins J, Napier JD, Sreedasyam A, Healey A, Session A, Shu S *et al.* 2021. Genomic mechanisms of climate adaptation in polyploid bioenergy switchgrass. *Nature* **590**: 438–444.

Lu Z, Yu H, Xiong G, Wang J, Jiao Y, Liu G, Jing Y, Meng X, Hu X, Qian Q *et al.* 2013. Genome-wide binding analysis of the transcription activator ideal plant architecture1 reveals a complex network regulating rice plant architecture. *Plant Cell* **25**: 3743–3759.

Luo L, Li W, Miura K, Ashikari M, Kyozuka J. 2012. Control of tiller growth of rice by *OsSPL14* and strigolactones, which work in two independent pathways. *Plant & Cell Physiology* **53**: 1793–1801.

Mann DGJ, LaFayette PR, Abercrombie LL, King ZR, Mazarei M, Halter MC, Poovaiah CR, Baxter H, Shen H, Dixon RA *et al.* 2012. Gateway-compatible vectors for high-throughput gene functional analysis in switchgrass (*Panicum*

virgatum L.) and other monocot species. *Plant Biotechnology Journal* **10**: 226–236.

Mashiguchi K, Sasaki E, Shimada Y, Nagae M, Ueno K, Nakano T, Yoneyama K, Suzuki Y, Asami T. 2009. Feedback-regulation of strigolactone biosynthetic genes and strigolactone-regulated genes in *Arabidopsis*. *Bioscience, Biotechnology, and Biochemistry* **73**: 2460–2465.

Mashiguchi K, Seto Y, Yamaguchi S. 2021. Strigolactone biosynthesis, transport and perception. *The Plant Journal* **105**: 335–350.

Mayzlish-Gati E, De-Cuyper C, Goormachtig S, Beeckman T, Vuylsteke M, Brewer PB, Beveridge CA, Yermiyahu U, Kaplan Y, Enzer Y *et al.* 2012. Strigolactones are involved in root response to low phosphate conditions in *Arabidopsis*. *Plant Physiology* **160**: 1329–1341.

Miura K, Ikeda M, Matsubara A, Song XJ, Ito M, Asano K, Matsuoka M, Kitano H, Ashikari M. 2010. *OsSPL14* promotes panicle branching and higher grain productivity in rice. *Nature Genetics* **42**: 545–549.

Omoarelojie LO, Kulkarni MG, Finnie JF, Van Staden J. 2019. Strigolactones and their crosstalk with other phytohormones. *Annals of Botany* **124**: 749–767.

Song X, Lu Z, Yu H, Shao G, Xiong J, Meng X, Jing Y, Liu G, Xiong G, Duan J *et al.* 2017. IPA1 functions as a downstream transcription factor repressed by D53 in strigolactone signaling in rice. *Cell Research* **27**: 1128–1141.

Sumanta N, Haque CI, Nishika J, Suprakash R. 2014. Spectrophotometric analysis of chlorophylls and carotenoids from commonly grown fern species by using various extracting solvents. *Research Journal of Chemical Sciences* **2231**: 606X.

Takeda T, Suwa Y, Suzuki M, Kitano H, Ueguchi-Tanaka M, Ashikari M, Matsuoka M, Ueguchi C. 2003. The *OsTB1* gene negatively regulates lateral branching in rice. *The Plant Journal* **33**: 513–520.

Thompson JF, Hayes LS, Lloyd DB. 1991. Modulation of firefly luciferase stability and impact on studies of gene regulation. *Gene* **103**: 171–177.

Varkonyi-Gasic E, Wu R, Wood M, Walton EF, Hellens RP. 2007. Protocol: a highly sensitive RT-PCR method for detection and quantification of microRNAs. *Plant Methods* **3**: 12.

Waldie T, McCulloch H, Leyser O. 2014. Strigolactones and the control of plant development: lessons from shoot branching. *The Plant Journal* **79**: 607–622.

Wang JW, Schwab R, Czech B, Mica E, Weigel D. 2008. Dual effects of miR156-targeted SPL genes and *CYP78A5/KLUH* on plastochron length and organ size in *Arabidopsis thaliana*. *Plant Cell* **20**: 1231–1243.

Wang L, Wang B, Yu H, Guo H, Lin T, Kou L, Wang A, Shao N, Ma H, Xiong G *et al.* 2020. Transcriptional regulation of strigolactone signalling in *Arabidopsis*. *Nature* **583**: 277–281.

Waters MT, Gutjahr C, Bennett T, Nelson DC. 2017. Strigolactone signaling and evolution. *Annual Review of Plant Biology* **68**: 291–322.

Wu G, Poethig RS. 2006. Temporal regulation of shoot development in *Arabidopsis thaliana* by miR156 and its target *SPL3*. *Development* **133**: 3539–3547.

Wu Z, Cao Y, Yang R, Qi T, Hang Y, Lin H, Zhou G, Wang ZY, Fu C. 2016. Switchgrass SBP-box transcription factors *PvSPL1* and *2* function redundantly to initiate side tillers and affect biomass yield of energy crop. *Biotechnology for Biofuels* **9**: 101.

Xi YJ, Fu C, Ge YX, Nandakumar R, Hisano H, Bouton J, Wang ZY. 2009. Agrobacterium-mediated transformation of switchgrass and inheritance of the transgenes. *BioEnergy Research* **2**: 275–283.

Xie K, Wu C, Xiong L. 2006. Genomic organization, differential expression, and interaction of SQUAMOSA promoter-binding-like transcription factors and microRNA156 in rice. *Plant Physiology* **142**: 280–293.

Yoneyama K, Akiyama K, Brewer PB, Mori N, Kawano-Kawada M, Haruta S, Nishiwaki H, Yamauchi S, Xie X, Umehara M *et al.* 2020. Hydroxyl carlactone derivatives are predominant strigolactones in *Arabidopsis*. *Plant Direct* **4**: e00219.

Yoneyama K, Brewer PB. 2021. Strigolactones, how are they synthesized to regulate plant growth and development? *Current Opinion in Plant Biology* **63**: 102072.

Yoneyama K, Mori N, Sato T, Yoda A, Xie X, Okamoto M, Iwanaga M, Ohnishi T, Nishiwaki H, Asami T *et al.* 2018. Conversion of carlactone to carlactonoic acid is a conserved function of MAX1 homologs in strigolactone biosynthesis. *The New Phytologist* **218**: 1522–1533.

Yoneyama K, Xie X, Yoneyama K, Takeuchi Y. 2009. Strigolactones: structures and biological activities. *Pest Management Science* **65**: 467–470.

Zhou F, Lin Q, Zhu L, Ren Y, Zhou K, Shabek N, Wu F, Mao H, Dong W, Gan LU *et al.* 2013. D14-SCF(D3)-dependent degradation of D53 regulates strigolactone signalling. *Nature* **504**: 406–410.

Zhang Y, van Dijk ADJ, Scaffidi A, Flematti GR, Hofmann M, Charnikhova T, Verstappen F, Hepworth JO, van der Krol S, Leyser O *et al.* 2014. Rice cytochrome P450 MAX1 homologs catalyze distinct steps in strigolactone biosynthesis. *Nature Chemical Biology* **10**: 1028–1033.

Zhang X, Madi S, Borsuk L, Nettleton D, Elshire RJ, Buckner B, Janick-Buckner D, Beck J, Timmermans M, Schnable PS *et al.* 2007. Laser microdissection of narrow sheath mutant maize uncovers novel gene expression in the shoot apical meristem. *PLoS Genetics* **3**: e101.

Supporting Information

Additional Supporting Information may be found online in the Supporting Information section at the end of the article.

Fig. S1 Morphological characterization of the control and miR156$_{OE}$ transgenic switchgrass plants.

Fig. S2 Phenotypic characterizations of the control and LBO$_{OEI}$ transgenic switchgrass plants.

Fig. S3 Comparison of the leaves and internodes harvested from control and LBO$_{OEII}$ plants.

Fig. S4 Analysis of the expression levels of SL-related genes in the control and LBO$_{OE}$ transgenic switchgrass plants.

Fig. S5 Downregulation of *PvLBO* produced axillary shoots at some nodes.

Fig. S6 Gross morphologies of the LBO$_{RNAi}$ and LBO$_{OE}$ transgenic switchgrass plants after treatment with 2 μM *rac*-GR24 and 4 μM TIS108, respectively.

Fig. S7 Gene ontology enrichment of differentially expressed genes.

Fig. S8 The contents of carotenoid and chlorophyll in the control, LBO$_{OEI}$, LBO$_{OEII}$, and LBO$_{RNAi}$ transgenic switchgrass plants.

Fig. S9 Differentially expressed lignin-related genes in LBO$_{OE}$ transgenic switchgrass plants.

Fig. S10 The contents of AcBr lignin in the control, LBO$_{OEI}$, LBO$_{OEII}$, and LBO$_{RNAi}$ transgenic switchgrass plants.

Fig. S11 Expression levels of strigolactone biosynthetic and signaling genes in SPL2$_{OE}$ transgenic switchgrass.

Fig. S12 *PvLBO* expression was activated by PvSPL4.

Fig. S13 Interaction between PvSPL2 and PvD53.

Table S1 List of primer pairs used in this study.

Table S2 Amino acid sequences of LBO in different plant species.

Table S3 Probe sequences for luciferase reporter and yeast one-hybrid assays.

Table S4 Upregulated genes in $PvLBO_{OE}$ RNA-Seq libraries compared to the control.

Table S5 Downregulated genes in $PvLBO_{OE}$ RNA-Seq libraries compared to the control.

Table S6 The differentially expressed SL-related genes in the LBO_{OE} RNA-Seq libraries.

Please note: Wiley Blackwell are not responsible for the content or functionality of any Supporting Information supplied by the authors. Any queries (other than missing material) should be directed to the *New Phytologist* Central Office.